Short Article

Molecular Cell

Hsp90 Breaks the Deadlock of the Hsp70 Chaperone System

Graphical Abstract

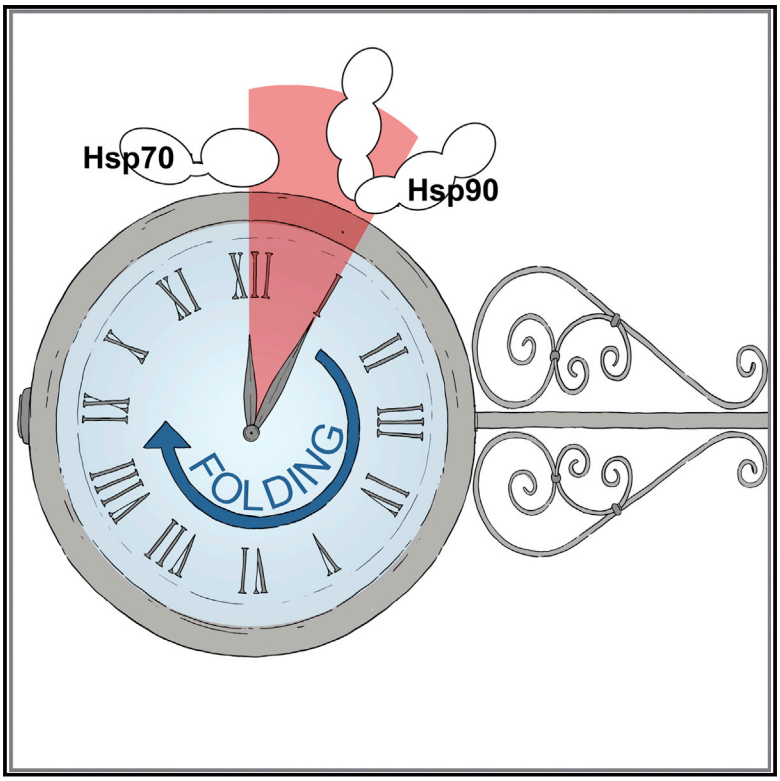

Authors

Tania Morán Luengo, Roman Kityk, Matthias P. Mayer, Stefan G.D. Rüdiger

Correspondence

m.mayer@zmbh.uni-heidelberg.de (M.P.M.), s.g.d.rudiger@uu.nl (S.G.D.R.)

In Brief

Chaperones help proteins to fold into their native state. Here, Morán Luengo et al. show that, contrary to expectations, the chaperone Hsp70 can block protein folding and that Hsp90 relieves the block to restart the folding reaction.

Highlights

- At physiological concentration, Hsp70 blocks effective protein folding
- Hsp90 restarts folding, overcoming the Hsp70-inflicted folding block
- The Hsp70-Hsp90 cascade increases folding yields, but does not alter folding kinetics
- Short ATP depending chaperone phase is followed by slow Anfinsen folding

Morán Luengo et al., 2018, Molecular Cell *70*, 545–552
May 3, 2018
https://doi.org/10.1016/j.molcel.2018.03.028

CellPress

Molecular Cell
Short Article

Hsp90 Breaks the Deadlock of the Hsp70 Chaperone System

Tania Morán Luengo,[1,2] Roman Kityk,[3] Matthias P. Mayer,[3,*] and Stefan G.D. Rüdiger[1,2,4,*]
[1]Cellular Protein Chemistry, Bijvoet Center for Biomolecular Research, Utrecht University, Padualaan 8, 3584 CH Utrecht, the Netherlands
[2]Science for Life, Utrecht University, Padualaan 8, 3584 CH Utrecht, the Netherlands
[3]Center for Molecular Biology of Heidelberg University (ZMBH), DKFZ-ZMBH-Alliance, Im Neuenheimer Feld 282, 69120 Heidelberg, Germany
[4]Lead Contact
*Correspondence: m.mayer@zmbh.uni-heidelberg.de (M.P.M.), s.g.d.rudiger@uu.nl (S.G.D.R.)
https://doi.org/10.1016/j.molcel.2018.03.028

SUMMARY

Protein folding in the cell requires ATP-driven chaperone machines such as the conserved Hsp70 and Hsp90. It is enigmatic how these machines fold proteins. Here, we show that Hsp90 takes a key role in protein folding by breaking an Hsp70-inflicted folding block, empowering protein clients to fold on their own. At physiological concentrations, Hsp70 stalls productive folding by binding hydrophobic, core-forming segments. Hsp90 breaks this deadlock and restarts folding. Remarkably, neither Hsp70 nor Hsp90 alters the folding rate despite ensuring high folding yields. In fact, ATP-dependent chaperoning is restricted to the early folding phase. Thus, the Hsp70-Hsp90 cascade does not fold proteins, but instead prepares them for spontaneous, productive folding. This stop-start mechanism is conserved from bacteria to man, assigning also a general function to bacterial Hsp90, HtpG. We speculate that the decreasing hydrophobicity along the Hsp70-Hsp90 cascade may be crucial for enabling spontaneous folding.

INTRODUCTION

It is the primary sequence of the protein that determines its native fold (Anfinsen, 1973). Proteins condense around an initial nucleus, the hydrophobic core, and ultimately fold into the same structure each time (Daggett and Fersht, 2003). Recapitulating protein folding *in vitro* usually requires conditions that are far away from physiological states. In the cell, conserved families of molecular chaperones support folding of proteins in an energy-consuming manner, presumably by repeated cycles of binding and release (Buchberger et al., 2010; Ellis, 1987; Kim et al., 2013; Mayer, 2013). The non-native polypeptide substrates targeted by chaperones are also known as clients. The molecular determinants of assisted protein folding, however, remain largely enigmatic.

The ubiquitous, ATP-dependent Hsp70 chaperone interacts with virtually all unfolded or misfolded proteins and has been demonstrated to refold numerous proteins into their native state. The likewise ATP-dependent Hsp90 chaperone is believed to be more specific, targeting certain proteins in a near-native state (Jakob et al., 1995; Karagöz and Rüdiger, 2015; Li et al., 2012; Taipale et al., 2012). Hsp90 acts downstream of Hsp70, but its contribution to protein folding is unclear (Karagöz et al., 2014; Karagöz and Rüdiger, 2015). Hsp70 and Hsp90 work together to promote maturation of steroid receptors in an ATP-dependent manner (Kirschke et al., 2014; Sanchez et al., 1987; Smith et al., 1992), and the co-chaperone Hop physically links both chaperones, facilitating substrate transfer from Hsp70 to Hsp90 (Wegele et al., 2006). Hsp90 is suggested to remodel the client downstream of Hsp70, but its impact on the folding yield is marginal, and its molecular role remains enigmatic (Genest et al., 2011, 2015).

Indeed, Hsp70 can refold proteins in the absence of Hsp90 (Schröder et al., 1993). However, two issues appeared paradoxical to us. First, Hsp70 promotes protein folding while it binds to short, very hydrophobic stretches, which are required to form the hydrophobic core of the protein (Rüdiger et al., 1997; Karagöz et al., 2014). Second, Hsp70 is also required to bind with high association rate, within seconds, to outcompete their high aggregation propensity (Mayer et al., 2000; Mayer and Bukau, 2005). How can hydrophobic cores form when Hsp70 binds to the very stretches that are required for folding, and how do complex proteins form their hydrophobic core and ultimately reach the native state in the presence of fast-rebinding Hsp70?

Here, we propose that the chaperone machines Hsp70 and Hsp90 form a conserved cascade that promotes spontaneous protein folding by a stop-start mechanism. Instead of refolding proteins, Hsp70 blocks folding when present at physiological concentrations. It is the transfer of the client to Hsp90 that is crucial to break the deadlock and to allow the protein to start a productive folding trajectory. Our findings describe the mode of action of the Hsp70-Hsp90 cascade and thus provide molecular understanding of chaperone-assisted protein folding.

RESULTS

Hsp70 Inhibits Substrate Refolding

Protein folding activity of Hsp70 chaperones was established both *in vivo* and *in vitro* using luciferase as a paradigmatic client, *nota bene* in the absence of Hsp90 (Schröder et al., 1993). To

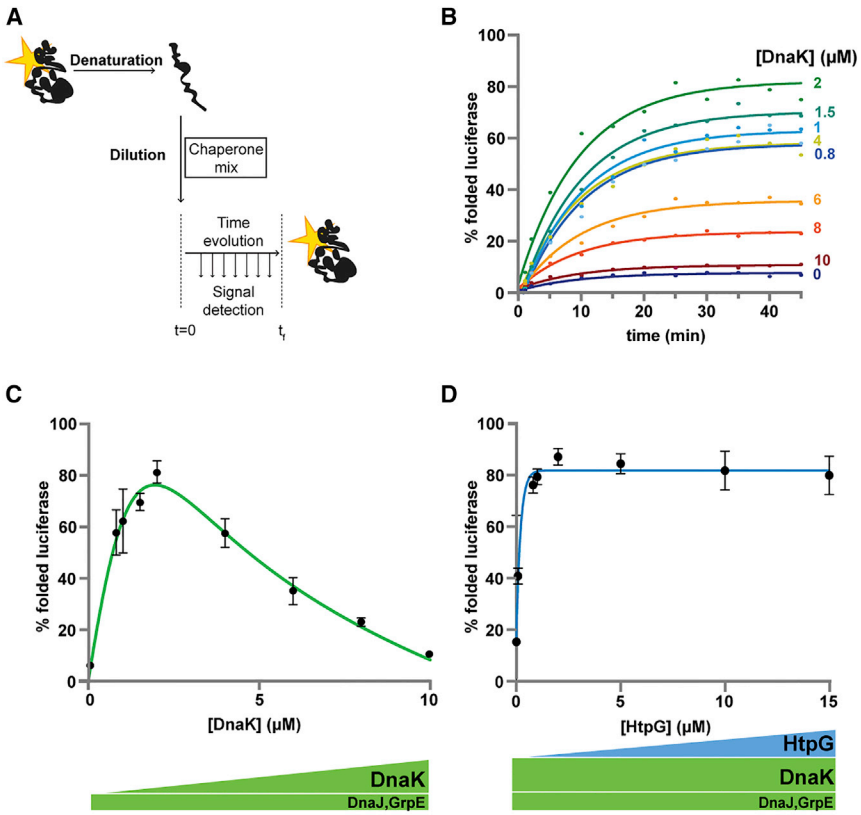

Figure 1. Hsp90 Rescues Luciferase out of the Hsp70 Trap

(A) Experimental setup.

(B) Time course of luciferase refolding in the presence of constant levels of DnaJ (160 nM) and GrpE (400 nM) and increasing concentrations of DnaK (blue to red, 0 to 10 μM), fitted as a first-order reaction with identical rates.

(C) High concentrations of DnaK inhibit luciferase refolding. Plateau refolding yields in (B) were plotted against DnaK concentration (±SEM), and data were fitted as shown in the STAR Methods section and explained in detail in the Equation System.

(D) Reactivation of denatured luciferase at 10 μM DnaK levels as a function of HtpG concentration (±SD of plateau).

understand the chaperone activity of Hsp70, we first revisited refolding of luciferase by the *E. coli* Hsp70 system. This consists of the Hsp70 DnaK, the ATPase-stimulating J-protein DnaJ, and the nucleotide exchange factor GrpE. We confirmed the seminal findings of the Bukau laboratory that luciferase refolds in the presence of the Hsp70 system.

Substrate proteins bind to DnaK at high rates, within seconds, but folding of, for example, luciferase takes around 30 min (Hu et al., 2006; Kityk et al., 2015; Schröder et al., 1993). Increasing Hsp70 levels should further favor the association of Hsp70 with an unfolding protein, so that chaperone activity may possibly compete with productive folding. We therefore chemically denatured luciferase and monitored the refolding rate in the presence of the Hsp70 system (Figure 1A). We kept the concentration of luciferase, DnaJ, and GrpE constant and titrated DnaK. We observed that independent of chaperone levels, the activity of refolded luciferase reaches a plateau after around 30 min (Figure 1B). The refolding yield, however, depended strongly on the concentration of Hsp70. Refolded luciferase increased to a maximum of 82% refolded luciferase at 2 μM DnaK. Strikingly, however, increasing Hsp70 levels further successively reduced the yield, dropping eventually to background levels at 10 μM DnaK (Figure 1C). Thus, Hsp70 is not only a promoter but also an effective inhibitor of folding of luciferase.

This phenomenon depends only on the levels of Hsp70 itself and not on the relative ratio of chaperone to co-chaperones. A similar picture was revealed when titrating DnaK, DnaJ, and GrpE together: a maximal refolding yield of 83.5% was reached at 5 μM DnaK, subsequently falling to background levels at 10 μM (Figures 2A and 2B). The physiological concentration of *E. coli* Hsp70 is even higher (~27 μM at 30°C) and doubles upon heat shock (Mogk et al., 1999). A 10-fold increase in luciferase levels did not release the Hsp70 block (Figure 2C). The Hsp70 block thus depends on the absolute Hsp70 levels, not on the ratio of Hsp70 to substrate. Together, these results suggest that Hsp70 requires an additional factor for effective refolding at physiological concentrations.

Hsp90 Restores Folding Yields at High Hsp70 Levels

Given that Hsp90 acts downstream of Hsp70, we considered whether *E. coli* Hsp90 (HtpG) would restore the folding activity at physiological Hsp70 levels (Karagöz and Rüdiger, 2015). Hsp90 acts on steroid receptors downstream of Hsp70, and *E. coli* Hsp90, HtpG, was found to have a mild effect on DnaK-dependent luciferase refolding (Genest et al., 2011, 2015; Kirschke et al., 2014; Sanchez et al., 1987). Here, we found that at high levels of the Hsp70 system, Hsp90 dramatically restored the folding capacity to maximum levels, increasing the folding yield from less than 10% to more than 80%, even when substoichiometric to Hsp70 (1 μM HtpG restores folding in the presence of 10 μM DnaK; Figures 1D and 2D). Importantly, and in contrast to Hsp70, high levels of Hsp90 (15 μM) were not detrimental to folding. Thus, Hsp90 becomes essential for folding at high Hsp70 levels, without adverse side effects at physiological concentrations.

Since Hsp90 is essential for folding at high Hsp70 levels, we explored whether Hsp90 functions as a safeguard, making the Hsp70 system robust to fluctuation in free chaperone levels, as naturally occurs upon and after cell stress. In the presence of Hsp90 (1 μM HtpG), we titrated the *E. coli* Hsp70 system up to physiological levels (27.4 μM DnaK/1 μM DnaJ/6.2 μM GrpE). The yield of refolded protein reached a plateau above 5 μM DnaK (Figure 2E). Thus, Hsp90 ensures that folding efficiency is independent of the levels of free Hsp70 and its co-chaperones.

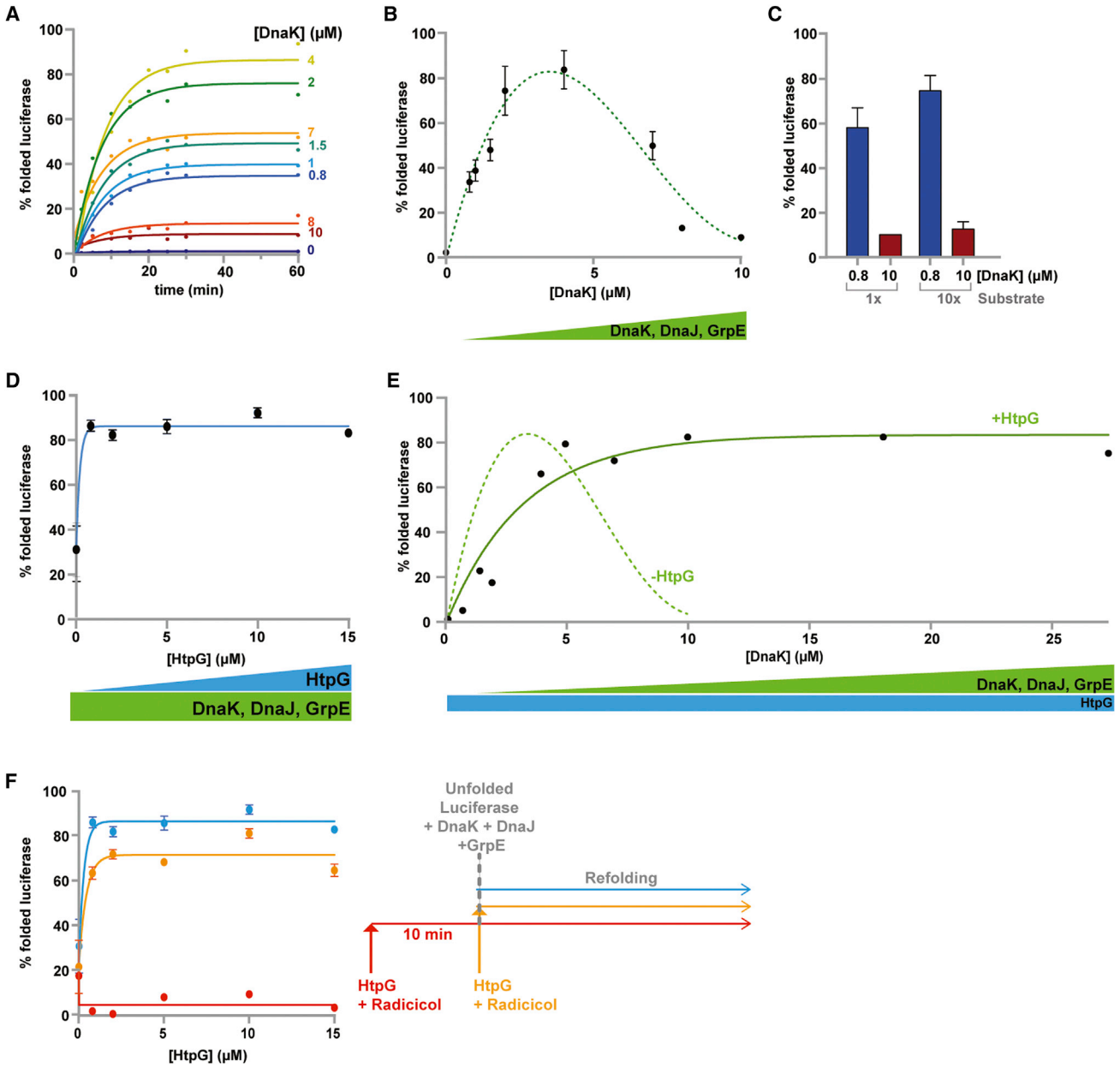

Figure 2. Hsp90 Buffers the Hsp70 System in an ATP-Dependent Way

(A) Time course of luciferase refolding in the presence of increasing DnaK/DnaJ/GrpE concentrations keeping a constant molar ratio (10:2:5). Fitting as in Figure 1B.

(B) Plateau refolding yields in (A) plotted against DnaK concentration (±SEM).

(C) Hsp70 folding block is independent of the chaperone/substrate ratio. Low DnaK concentration (blue, 0.8 μM) and high (red, 10 μM) show similar results at 80 nM or 800 nM of luciferase (±SEM).

(D) Reactivation of denatured luciferase at high DnaK/DnaJ/GrpE levels as a function of HtpG concentration (±SD of plateau).

(E) Titration of DnaK/DnaJ/GrpE keeping a constant ratio (10:2:5) in the presence of HtpG (1 μM). Data from (B) were used for comparison (dotted line).

(F) ATPase activity is required for substrate rescuing from DnaK. HtpG titration at high levels of DnaK/DnaJ/GrpE (10:2:5 μM; blue, no radicicol; orange, 30 μM radicicol; red, 30 μM radicicol pre-bound to Hsp90 [±SD of plateau]). The scheme on the right explains the timing of addition.

In the absence of Hsp70, however, Hsp90 alone does not refold luciferase (Figure 2E).

ATP-Dependent Chaperoning in Early Stages

Hsp90 activity is linked to ATP hydrolysis, which is required to take over the client from Hsp70 (Kirschke et al., 2014; Prodromou et al., 1997). To determine the timing of ATPase action of Hsp90, we added the Hsp90-specific, ATP-competitive inhibitor radicicol to the assay. Radicicol blocked Hsp90 folding activity, consistent with earlier findings (Genest et al., 2011) (Figure 2F). Remarkably, radicicol prevented substrate takeover by Hsp90 only when pre-incubated with the chaperone. As radicicol binds

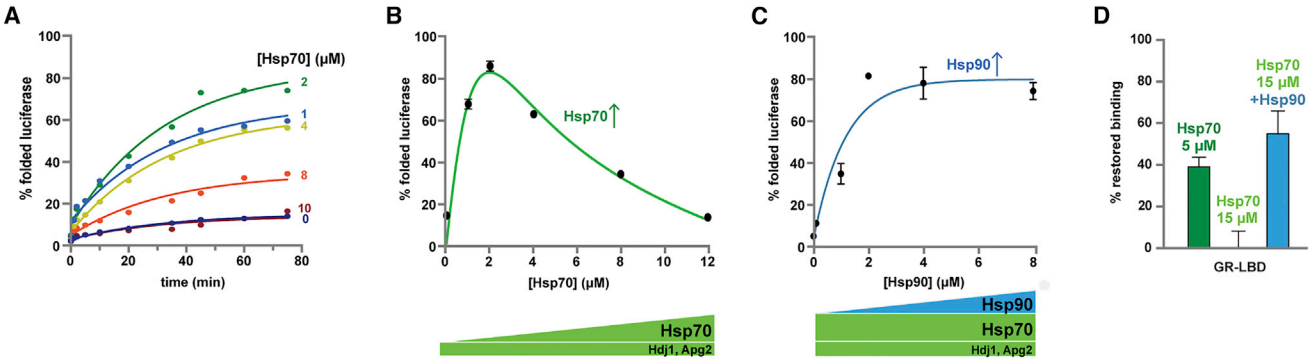

Figure 3. The Effect of Hsp90 on the Hsp70 System Is Conserved and Substrate Independent

(A) Time course of luciferase refolding at constant levels of Hdj1 (1 μM) and Apg2 (200 nM) and increasing Hsp70 (blue to red, 0 to 12 μM) fitted as a first-order reaction with identical rates.

(B) High Hsp70 levels inhibit luciferase refolding. Plateau refolding yields were plotted against Hsp70 concentration (±SD of plateau), and data were fitted as shown in the STAR Methods. Physiological levels of Hsp70 in different cell lines are shown in Table S1.

(C) Hsp90 rescues luciferase refolding at high Hsp70 levels. Titration of Hsp90 and Hop keeping molar ratio (2:1) at constant high Hsp70/Hdj1/Apg2 levels (12:1:0.2 μM) (±SD of plateau).

(D) Normalized recovered binding of F-Dex to GR-LBD after thermal unfolding with chaperone components indicated (±SD).

quickly to Hsp90 (Phillips et al., 2007), these findings imply that the Hsp90 ATPase is only relevant in the earliest phase on the folding path. As the folding of luciferase continues for a further 30 min, this indicates that there is a short, initial period of chaperone action, after which folding of luciferase is independent of the ATPase activity of Hsp90. As Hsp90 acts downstream of Hsp70, this finding suggests that chaperoning is restricted to the first few seconds of the folding path. The largest part is free of ATP-dependent chaperone activity and thus chaperone-free.

The Mechanism Is Conserved across Species

To elucidate whether the interplay between the bacterial Hsp70 and Hsp90 systems is a conserved process, we repeated the experiments with the human chaperones. We confirmed that, assisted by the J-protein Hdj1 and the nucleotide exchange factor Apg2, human Hsp70 (HSPA1A) is able to refold luciferase (Figure 3A) (Freeman and Morimoto, 1996; Rampelt et al., 2012). We monitored luciferase refolding in the presence of increasing concentrations of all three members of the Hsp70 system (Figures 3A and 3B). At 2 μM Hsp70, refolding of luciferase was maximal (75%). Further increase of Hsp70 concentration subsequently reduced refolding efficiency until basal refolding levels were reached at 12 μM Hsp70. Notably, the concentration of Hsp70 in eukaryotic cells is around 18 μM (Geiger et al., 2012; Stankiewicz et al., 2010) (Table S1). However, addition of Hsp90 and the Hsp70-Hsp90 adaptor protein Hop at high Hsp70 concentrations restored folding of luciferase in a substoichiometric manner (Figure 3C). This indicates that the function of Hsp90 chaperones to counter the Hsp70-inflicted folding block is conserved between bacteria and man.

Folding Rate Is Chaperone Independent

We wondered whether the chaperones affected the folding rate of luciferase. In fact, the association rate of DnaK is much higher than the folding rate of the client. The association rate (k_{ON}) for peptides to DnaK in the ATP state is $\sim 10^6$ M^{-1} s^{-1} (Mayer et al., 2000; Schmid et al., 1994), and the $T_{1/2}$ for folding of luciferase with the DnaK system 6–8 min (~400 s). Thus, at the concentrations of our assay, DnaK is constantly binding to luciferase (~1 s^{-1} at the lowest concentration and 10 s^{-1} at the highest). During folding, DnaK can re-bind luciferase multiple times and presumably in different sites before it reaches the native state, which at high DnaK concentration translates into inhibition of the folding process. Therefore, we developed an equation system (see STAR Methods) to take the dynamic nature and the fast and multiple binding of Hsp70 to the client into account and analyzed the luciferase refolding curves.

Remarkably, in all experiments, the folding rate of luciferase always followed first-order kinetics (averaged rates $5 \pm 2 \times 10^{-4}$ s^{-1} for 0–10 μM Hsp70 [Figure 2A] and $6 \pm 4 \times 10^{-4}$ s^{-1} for 0–8 μM Hsp90 [Figure 2D]). First-order kinetics indicate that the reaction depends on the concentration of the folding protein itself; however, neither presence nor concentration of any chaperone tested in this study significantly influenced the folding rate (Figures 1, 2, and 3). We concluded that although the chaperones dramatically improved the refolding yield, they did not change the refolding rate and thus not the transition state on the folding path. This is consistent with Anfinsen's thermodynamic hypothesis for protein folding (Anfinsen, 1973). Thus, neither Hsp70 nor Hsp90 actively contribute to the folding process of luciferase. Therefore, the Hsp70-Hsp90 cascade lacks foldase activity, despite being required to generate high yields of refolded protein.

A key reason for Hsp70 to inhibit the folding of luciferase could be multiple simultaneous binding events. This is consistent with earlier findings that potential binding sites for Hsp70 exist on average every 30–40 residues (Rüdiger et al., 1997). Since an average protein in *E. coli* has about 360 residues, and an average eukaryotic protein has about 500 residues, these proteins have on average 10–15 sites Hsp70 can bind. Our data are consistent with several Hsp70 molecules binding simultaneously a single client polypeptide chain (see Scheme 1, STAR Methods), as had been shown by molecular simulations and NMR experiments (Kellner et al., 2014, Rosenzweig et al., 2017). Since Hsp70 dissociation is a stochastic and concentration-independent process,

whereas Hsp70 binding to the client is concentration dependent, above a certain Hsp70 concentration, rebinding will occur at higher rates than dissociation. Folding of the client, however, would require all hydrophobic sites to be simultaneously available for the formation of the hydrophobic core. Thus, Hsp70 rebinding may prevent folding of the protein. Notably, we could fit the Hsp70-dependent folding block when assuming that up to three Hsp70 may bind to the client, converting it into an irreversible state, e.g., when re-association of Hsp70 occurs at higher rates than dissociation (Figures 1B and 3B).

Mechanism Is Client Independent

This led us to test whether the mechanisms established here using luciferase could be confirmed for a classical Hsp90 *in vivo* and *in vitro* client, the ligand binding domain of the glucocorticoid receptor (GR-LBD) (Kirschke et al., 2014; Lorenz et al., 2014; Sanchez et al., 1987). Folding of GR-LBD can be monitored by binding to a fluorescent-labeled hormone derivative (Kirschke et al., 2014; Lorenz et al., 2014). After thermally unfolding GR-LBD, we monitored refolding at permissive temperature in the presence of Hsp70 and Hsp90. At a high concentration of Hsp70 (15 μM) and in line with previous findings, Hsp90 (together with its co-chaperone Hop) strictly controlled refolding (Kirschke et al., 2014; Sanchez et al., 1987). At a low Hsp70 concentration (5 μM), however, Hsp90 was not essential for GR-LBD folding (Figure 3D). We conclude that the mechanistic interplay of Hsp70 and Hsp90 is also valid for folding of this paradigmatic steroid hormone receptor, which requires Hsp90 for maturation in the cell.

DISCUSSION

Here, we identify the key of the function of Hsp90 in protein folding as resolving the Hsp70-imposed folding deadlock. This block is intrinsically linked to the specificity of Hsp70 for core-forming polypeptide segments. Hsp90 binding enables proteins to complete the early nucleation phase and to re-start the stalled folding trajectory, which ultimately leads to the native state. We find this to be a conserved and general function generating an Hsp70-Hsp90 cascade robust against fluctuations in chaperone levels and co-chaperone ratios. Remarkably, neither Hsp70 nor Hsp90 alter the folding rate, despite dramatically increasing the folding yield. Together, our findings suggest a molecular mechanism through which Hsp90 improves the folding efficiency of the Hsp70 machine.

Evolution of Chaperoned Folding

Hsp90 can act downstream of Hsp70 (Genest et al., 2011, 2015; Nakamoto et al., 2014; Pratt and Toft, 2003; Schumacher et al., 1996; Wegele et al., 2006). The nature of this activity has been elusive, as Hsp90 showed only minor effects on folding yields, contrasting its essential function in maturation processes for many regulatory proteins (Genest et al., 2011; Kirschke et al., 2014; Pratt and Toft, 1997). As we show here, the presence of Hsp90 ensures permanent high folding yields (Figure 2E), generating a machinery that is reliable even upon dramatic increase in Hsp70 levels under heat shock conditions. We conclude that there is no systematic difference between the functions of Hsp90 in protein maturation and in folding.

The components of the Hsp70-Hsp90 cascade are conserved in the cytosol from bacteria to man and are present in the main folding organelles of higher eukaryotes (Johnson, 2012). Hsp70 and Hsp90 collaborate by direct interaction, further assisted by the co-chaperone Hop in eukaryotes (Genest et al., 2015; Kravats et al., 2018; Wegele et al., 2006; Alvira et al., 2014). This cascade thus takes a major role in assisted protein folding throughout all kingdoms of life. The function of Hsp90 in this cascade is that of an optimizer, at least for such diverse clients as heterologous luciferase and homologous GR.

Hsp90 is essential neither in *E. coli* nor in the ER or mitochondria of eukaryotes (Johnson, 2012). We expect that proteins may escape the Hsp70 deadlock in other ways, although this is likely to be less efficient. We speculate that new supply of nascent chains or unfolded protein under stress conditions may contribute to break the Hsp70 deadlock in the absence of Hsp90. Otherwise, Hsp70 may also be inactivated by, for instance, oligomerization or posttranslational modification, like BiP (the Hsp70 ER paralog) inactivation by AMPylation (Preissler et al., 2017). The re-start activity of Hsp90 may be particularly crucial for slow-folding, complex proteins, making this chaperone essential in the cytoplasm of higher eukaryotes as well as in certain bacteria under heat stress (Honoré et al., 2017).

Protective Role of Hsp90

Hsp90 activity is particularly important for kinases in need of their activator proteins and steroid hormone receptors requiring their ligands (Huse and Kuriyan, 2002; Schopf et al., 2017). Lacking these factors, the intermediate species might remain bound to Hsp90 for longer, in a folding-competent conformation. In that case, certain co-chaperones might be needed to stall Hsp90 activity and maintain this folding-upon-activation state (Radli and Rüdiger, 2017; Sahasrabudhe et al., 2017). Such a stalled Hsp90-bound intermediate is seen in the structural model of Cdk4 in complex with Hsp90-Cdc37 (Verba et al., 2016). This protective role explains the increased folding dependence of disease-causing mutant proteins on Hsp90 (Karras et al., 2017). In the case of particularly unstable kinases and transcription factors, Hsp90 is needed for the stability of the mature protein (Xu et al., 2001). Hsp90 inhibition causes destabilization and misfolding of the client, which may subsequently bind Hsp70 through their now-exposed hydrophobic residues. The client then remains in the deadlock of Hsp70 chaperone cycles until co-chaperones like the ubiquitin ligase CHIP bind to Hsp70 and target the client for proteasomal degradation (Johnson and Toft, 1995; Stankiewicz et al., 2010; Xu et al., 2002).

Chaperoned Energy Landscape

Our data suggest that neither Hsp70 nor Hsp90 actively (re-)fold the client. This is in line with previous observations that the ATPase activity of DnaK is required for an early unfolding reaction, but not for subsequent folding (Sharma et al., 2010). Accordingly, we show that folding kinetics are independent of the chaperone concentration, implying that chaperone action takes place at an early stage, in the formation of the protein nucleus, and that chaperone-free folding is the rate-limiting step of the reaction. Additionally, our data indicate that Hsp90 acts more quickly than the inhibitor radicicol can bind (Figure 2F). Taken together, these findings strongly suggest that the Hsp70-Hsp90 cascade acts prior to

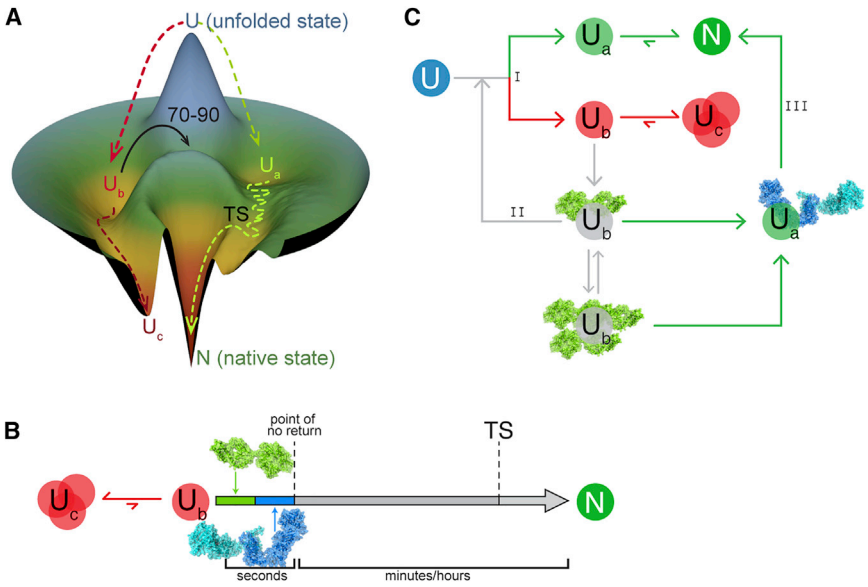

Figure 4. General Model for Chaperoned Protein Folding

(A) Three-dimensional scheme for protein folding. Energy landscape shows the effect of chaperones in early stages. U_b, a misfolded intermediate, is boosted by chaperones to a state that allows self-evolution following a slow path toward the native state.

(B) Time scheme indicating the action of the Hsp70/Hsp90 cascade early on the folding path, far ahead of the transition state.

(C) Chaperone-assisted folding mechanism. Unfolded protein directly evolves into two states, folding-competent U_a and aggregation/misfolding-prone U_b, which binds to Hsp70. After release from Hsp70, the protein can further evolve to U_a or U_b. However, high Hsp70 levels inhibit the return to the U_a/U_b junction. Hsp90 removes the Hsp70-inflicted folding block, promoting progression to the native state. Roman numbers indicate the three modes proposed for protein folding (I, spontaneous folding; II, Hsp70 cycling; III, Hsp70-Hsp90 cascade). See also Figure S1.

the transition state of the client folding reaction. Based on the discussed facts, we propose that the unfolded client (U), ensemble of rapidly interconverting structures (Fersht and Daggett, 2002), can evolve from its unstable state through two different ways: U_a, an on-pathway intermediate that can eventually reach the native state, and U_b, an off-pathway species prone to aggregation and able to bind to chaperones. The task of the folding cascade is repositioning the folding client on the energy hypersurface such that it can ultimately fold autonomously according to Anfinsen, independent of chaperone action. A tridimensional illustration of this concept is presented in Figure 4A, and the chronological pathway is shown in Figure 4B.

Folding Scheme Hsp70-Hsp90 Cascade

Combining current knowledge with the findings presented here, we propose a stop-start mechanism for cooperation of the Hsp70-Hsp90 cascade in protein folding (Figure 4C): (I) Independent from any chaperone, a fraction of the protein folds spontaneously; (II) in the presence of Hsp70 and absence of Hsp90, the protein cycles on Hsp70, allowing the protein to re-enter pathway I, a step blocked by excess of Hsp70; (III) in the presence of both Hsp70 and Hsp90, Hsp90 takes over from Hsp70, promoting folding by breaking the deadlock of unproductive cycling. Hsp90 provides a controlled restart of folding after Hsp70-assisted recovery of the client from the folding trap. Therefore, it may not be beneficial to continue repeated cycles of Hsp70 binding and release in the presence of Hsp90, making pathway III more efficient than pathway II. Involving Hsp90 in protein folding may thus be evolutionarily beneficial. The general function of Hsp90 in protein folding observed here is, we note, consistent with Hsp90 action in hormone receptor activation (Kirschke et al., 2014; Sanchez et al., 1987; Schowalter et al., 1991).

The function of Hsp70 is widely seen as foldase, notably a paradigm that has been established for luciferase (Freeman and Morimoto, 1996; Schröder et al., 1993; Liman et al., 2005; Kermer et al., 2015; Perales-Calvo et al., 2018). Although Hsp70 activity is indeed required to ensure high refolding yields of luciferase, our results show that at the molecular level, the Hsp70 system does not act as foldase. Why is Hsp90 needed to restart folding of an Hsp70-bound client? Given that the Hsp70 substrate binding pocket is highly hydrophobic, whereas the Hsp90 substrate binding site is much more hydrophilic (Karagöz and Rüdiger, 2015), we suggest that this gradient of decreasing hydrophobicity may be key in the functioning of the Hsp70-Hsp90 cascade. The more polar Hsp90 surface may stimulate the client to complete formation of its hydrophobic core, which cannot form while bound to Hsp70. In fact, a client can reach its native state while still bound to Hsp90 (Kirschke et al., 2014; Wegele et al., 2006). This may potentially be a widespread chaperone mechanism. The *E. coli* chaperonin GroEL recruits its substrate initially through a hydrophobic ring and, subsequent to capping by GroES, exposes the substrate protein to a larger and more hydrophilic chamber promoting folding (Xu et al., 1997). In an analogous way, Hsp90 would offer a more extended and less hydrophobic binding surface after the highly hydrophobic binding pocket of Hsp70 (Figure S1). Thus, exposure of the substrate to decreasing hydrophobicity may have a crucial role for client folding in general, particularly in the Hsp70-Hsp90 cascade.

STAR★METHODS

Detailed methods are provided in the online version of this paper and include the following:

- KEY RESOURCES TABLE
- CONTACT FOR REAGENT AND RESOURCE SHARING
- METHOD DETAILS
  - Protein Purification
  - Luciferase Refolding Assay
  - Luciferase Data Fitting
  - Equation System
  - GR-LBD Fluorescence Polarization Assay
- QUANTIFICATION AND STATISTICAL ANALYSIS

SUPPLEMENTAL INFORMATION

Supplemental Information includes one figure and one table and can be found with this article online at https://doi.org/10.1016/j.molcel.2018.03.028.

ACKNOWLEDGMENTS

We are grateful to Ineke Braakman for continuous support. We thank Friedrich Förster and Naomi Lodder for comments on the manuscript; Carlo van Mierlo, Daniel Fonseca, and Doron Gollnast for discussion; Bastiaan Schravendeel and Inés Arias García for graphical assistance; and Stefan Hennes and Elsbeth Schwarz for technical assistance. S.G.D.R. was supported by Marie-Curie Actions of the 7th Framework programme of the EU (Innovative Doctoral Programme "ManiFold" [No. 317371] and Initial Training Network "WntsApp" [No. 608180]), the Internationale Stichting Alzheimer Onderzoek (ISAO; project "Chaperoning Tau Aggregation"; No. 14542), and a ZonMW TOP grant ("Chaperoning Axonal Transport in neurodegenerative disease"; No. 91215084). This work was supported by the Deutsche Forschungsgemeinschaft (MA1278/4-3 to M.P.M.).

AUTHOR CONTRIBUTIONS

S.G.D.R. and M.P.M. conceived the study; S.G.D.R., M.P.M., and T.M.L. planned experiments; T.M.L. did experiments; T.M.L. and R.K. purified proteins and supported experiments; M.P.M. and T.M.L. analyzed data; S.G.D.R., M.P.M. and T.M.L. wrote the manuscript.

DECLARATION OF INTERESTS

The authors declare no competing interests.

Received: November 17, 2017
Revised: February 17, 2018
Accepted: March 23, 2018
Published: April 26, 2018

SUPPORTING CITATIONS

The following references appear in the Supplemental Information: Gillen and Forbush (1999); Hagemans et al. (2015); Krukenberg et al. (2011).

REFERENCES

Alvira, S., Cuéllar, J., Röhl, A., Yamamoto, S., Itoh, H., Alfonso, C., Rivas, G., Buchner, J., and Valpuesta, J.M. (2014). Structural characterization of the substrate transfer mechanism in Hsp70/Hsp90 folding machinery mediated by Hop. Nat. Commun. *5*, 5484.

Andréasson, C., Fiaux, J., Rampelt, H., Mayer, M.P., and Bukau, B. (2008). Hsp110 Is a Nucleotide-activated Exchange Factor for Hsp70. Journal of Biological Chemistry *283*, 8877–8884.

Anfinsen, C.B. (1973). Principles that govern the folding of protein chains. Science *181*, 223–230.

Bischofberger, P., Han, W., Feifel, B., Schönfeld, H.J., and Christen, P. (2003). D-Peptides as inhibitors of the DnaK/DnaJ/GrpE chaperone system. J. Biol. Chem. *278*, 19044–19047.

Buchberger, A., Schröder, H., Hesterkamp, T., Schönfeld, H.J., and Bukau, B. (1996). Substrate shuttling between the DnaK and GroEL systems indicates a chaperone network promoting protein folding. J. Mol. Biol. *261*, 328–333.

Buchberger, A., Bukau, B., and Sommer, T. (2010). Protein quality control in the cytosol and the endoplasmic reticulum: brothers in arms. Mol. Cell *40*, 238–252.

Daggett, V., and Fersht, A. (2003). The present view of the mechanism of protein folding. Nat. Rev. Mol. Cell Biol. *4*, 497–502.

Ellis, J. (1987). Proteins as molecular chaperones. Nature *328*, 378–379.

Fersht, A.R., and Daggett, V. (2002). Protein folding and unfolding at atomic resolution. Cell *108*, 573–582.

Freeman, B.C., and Morimoto, R.I. (1996). The human cytosolic molecular chaperones hsp90, hsp70 (hsc70) and hdj-1 have distinct roles in recognition of a non-native protein and protein refolding. EMBO J. *15*, 2969–2979.

Geiger, T., Wehner, A., Schaab, C., Cox, J., and Mann, M. (2012). Comparative proteomic analysis of eleven common cell lines reveals ubiquitous but varying expression of most proteins. Mol. Cell. Proteomics *11*, M111.014050.

Genest, O., Hoskins, J.R., Camberg, J.L., Doyle, S.M., and Wickner, S. (2011). Heat shock protein 90 from Escherichia coli collaborates with the DnaK chaperone system in client protein remodeling. Proc. Natl. Acad. Sci. USA *108*, 8206–8211.

Genest, O., Hoskins, J.R., Kravats, A.N., Doyle, S.M., and Wickner, S. (2015). Hsp70 and Hsp90 of E. coli Directly Interact for Collaboration in Protein Remodeling. J. Mol. Biol. *427*, 3877–3889.

Gillen, C.M., and Forbush, B., 3rd (1999). Functional interaction of the K-Cl cotransporter (KCC1) with the Na-K-Cl cotransporter in HEK-293 cells. Am. J. Physiol. *276*, C328–C336.

Graf, C., Stankiewicz, M., Kramer, G., and Mayer, M.P. (2009). Spatially and kinetically resolved changes in the conformational dynamics of the Hsp90 chaperone machine. EMBO J. *28*, 602–613.

Hagemans, D., van Belzen, I.A.M., Morán Luengo, T., and Rüdiger, S.G.D. (2015). A script to highlight hydrophobicity and charge on protein surfaces. Front. Mol. Biosci. *2*, 56.

Honoré, F.A., Méjean, V., and Genest, O. (2017). Hsp90 Is Essential under Heat Stress in the Bacterium Shewanella oneidensis. Cell Rep. *19*, 680–687.

Hu, B., Mayer, M.P., and Tomita, M. (2006). Modeling Hsp70-mediated protein folding. Biophys. J. *91*, 496–507.

Huse, M., and Kuriyan, J. (2002). The conformational plasticity of protein kinases. Cell *109*, 275–282.

Jakob, U., Lilie, H., Meyer, I., and Buchner, J. (1995). Transient interaction of Hsp90 with early unfolding intermediates of citrate synthase. Implications for heat shock in vivo. J. Biol. Chem. *270*, 7288–7294.

Johnson, J.L. (2012). Evolution and function of diverse Hsp90 homologs and cochaperone proteins. Biochim. Biophys. Acta *1823*, 607–613.

Johnson, J.L., and Toft, D.O. (1995). Binding of p23 and hsp90 during assembly with the progesterone receptor. Mol. Endocrinol. *9*, 670–678.

Karagöz, G.E., and Rüdiger, S.G.D. (2015). Hsp90 interaction with clients. Trends Biochem. Sci. *40*, 117–125.

Karagöz, G.E., Duarte, A.M.S., Akoury, E., Ippel, H., Biernat, J., Morán Luengo, T., Radli, M., Didenko, T., Nordhues, B.A., Veprintsev, D.B., et al. (2014). Hsp90-Tau complex reveals molecular basis for specificity in chaperone action. Cell *156*, 963–974.

Karras, G.I., Yi, S., Sahni, N., Fischer, M., Xie, J., Vidal, M., D'Andrea, A.D., Whitesell, L., and Lindquist, S. (2017). HSP90 Shapes the Consequences of Human Genetic Variation. Cell *168*, 856–866.e12.

Kellner, R., Hofmann, H., Barducci, A., Wunderlich, B., Nettels, D., and Schuler, B. (2014). Single-molecule spectroscopy reveals chaperone-mediated expansion of substrate protein. Proc. Natl. Acad. Sci. USA *111*, 13355–13360.

Kermer, P., Köhn, A., Schnieder, M., Lingor, P., Bähr, M., Liman, J., and Dohm, C.P. (2015). BAG1 is neuroprotective in in vivo and in vitro models of Parkinson's disease. J. Mol. Neurosci. *55*, 587–595.

Kim, Y.E., Hipp, M.S., Bracher, A., Hayer-Hartl, M., and Hartl, F.U. (2013). Molecular chaperone functions in protein folding and proteostasis. Annu. Rev. Biochem. *82*, 323–355.

Kirschke, E., Goswami, D., Southworth, D., Griffin, P.R., and Agard, D.A. (2014). Glucocorticoid receptor function regulated by coordinated action of the Hsp90 and Hsp70 chaperone cycles. Cell *157*, 1685–1697.

Kityk, R., Vogel, M., Schlecht, R., Bukau, B., and Mayer, M.P. (2015). Pathways of allosteric regulation in Hsp70 chaperones. Nat. Commun. *6*, 8308.

Kravats, A.N., Hoskins, J.R., Reidy, M., Johnson, J.L., Doyle, S.M., Genest, O., Masison, D.C., and Wickner, S. (2018). Functional and physical interaction between yeast Hsp90 and Hsp70. Proc. Natl. Acad. Sci. USA *115*, E2210–E2219.

Krukenberg, K.A., Street, T.O., Lavery, L.A., and Agard, D.A. (2011). Conformational dynamics of the molecular chaperone Hsp90. Q. Rev. Biophys. *44*, 229–255.

Laufen, T., Mayer, M.P., Beisel, C., Klostermeier, D., Mogk, A., Reinstein, J., and Bukau, B. (1999). Mechanism of regulation of hsp70 chaperones by DnaJ cochaperones. Proc. Natl. Acad. Sci. USA *96*, 5452–5457.

Li, J., Soroka, J., and Buchner, J. (2012). The Hsp90 chaperone machinery: conformational dynamics and regulation by co-chaperones. Biochim. Biophys. Acta *1823*, 624–635.

Liman, J., Ganesan, S., Dohm, C.P., Krajewski, S., Reed, J.C., Bähr, M., Wouters, F.S., and Kermer, P. (2005). Interaction of BAG1 and Hsp70 mediates neuroprotectivity and increases chaperone activity. Mol. Cell. Biol. *25*, 3715–3725.

Lorenz, O.R., Freiburger, L., Rutz, D.A., Krause, M., Zierer, B.K., Alvira, S., Cuéllar, J., Valpuesta, J.M., Madl, T., Sattler, M., and Buchner, J. (2014). Modulation of the Hsp90 chaperone cycle by a stringent client protein. Mol. Cell *53*, 941–953.

Malakhov, M.P., Mattern, M.R., Malakhova, O.A., Drinker, M., Weeks, S.D., and Butt, T.R. (2004). SUMO fusions and SUMO-specific protease for efficient expression and purification of proteins. J. Struct. Funct. Genomics *5*, 75–86.

Mayer, M.P. (2013). Hsp70 chaperone dynamics and molecular mechanism. Trends Biochem. Sci. *38*, 507–514.

Mayer, M.P., and Bukau, B. (2005). Hsp70 chaperones: cellular functions and molecular mechanism. Cell. Mol. Life Sci. *62*, 670–684.

Mayer, M.P., Schröder, H., Rüdiger, S., Paal, K., Laufen, T., and Bukau, B. (2000). Multistep mechanism of substrate binding determines chaperone activity of Hsp70. Nat. Struct. Biol. *7*, 586–593.

Mogk, A., Tomoyasu, T., Goloubinoff, P., Rüdiger, S., Röder, D., Langen, H., and Bukau, B. (1999). Identification of thermolabile Escherichia coli proteins: prevention and reversion of aggregation by DnaK and ClpB. EMBO J. *18*, 6934–6949.

Nakamoto, H., Fujita, K., Ohtaki, A., Watanabe, S., Narumi, S., Maruyama, T., Suenaga, E., Misono, T.S., Kumar, P.K., Goloubinoff, P., and Yoshikawa, H. (2014). Physical interaction between bacterial heat shock protein (Hsp) 90 and Hsp70 chaperones mediates their cooperative action to refold denatured proteins. J. Biol. Chem. *289*, 6110–6119.

Nguyen, M.T.N., Knieß, R.A., Daturpalli, S., Le Breton, L., Ke, X., Chen, X., and Mayer, M.P. (2017). Isoform-Specific Phosphorylation in Human Hsp90β Affects Interaction with Clients and the Cochaperone Cdc37. J. Mol. Biol. *429*, 732–752.

Perales-Calvo, J., Giganti, D., Stirnemann, G., and Garcia-Manyes, S. (2018). The force-dependent mechanism of DnaK-mediated mechanical folding. Sci. Adv. *4*, eaaq0243.

Phillips, J.J., Yao, Z.P., Zhang, W., McLaughlin, S., Laue, E.D., Robinson, C.V., and Jackson, S.E. (2007). Conformational dynamics of the molecular chaperone Hsp90 in complexes with a co-chaperone and anticancer drugs. J. Mol. Biol. *372*, 1189–1203.

Pratt, W.B., and Toft, D.O. (1997). Steroid receptor interactions with heat shock protein and immunophilin chaperones. Endocr. Rev. *18*, 306–360.

Pratt, W.B., and Toft, D.O. (2003). Regulation of signaling protein function and trafficking by the hsp90/hsp70-based chaperone machinery. Exp. Biol. Med. (Maywood) *228*, 111–133.

Preissler, S., Rohland, L., Yan, Y., Chen, R., Read, R.J., and Ron, D. (2017). AMPylation targets the rate-limiting step of BiP's ATPase cycle for its functional inactivation. eLife *6*, e29428.

Prodromou, C., Roe, S.M., O'Brien, R., Ladbury, J.E., Piper, P.W., and Pearl, L.H. (1997). Identification and structural characterization of the ATP/ADP-binding site in the Hsp90 molecular chaperone. Cell *90*, 65–75.

Radli, M., and Rüdiger, S.G.D. (2017). Picky Hsp90-Every Game with Another Mate. Mol. Cell *67*, 899–900.

Rampelt, H., Kirstein-Miles, J., Nillegoda, N.B., Chi, K., Scholz, S.R., Morimoto, R.I., and Bukau, B. (2012). Metazoan Hsp70 machines use Hsp110 to power protein disaggregation. EMBO J. *31*, 4221–4235.

Rosenzweig, R., Sekhar, A., Nagesh, J., and Kay, L.E. (2017). Promiscuous binding by Hsp70 results in conformational heterogeneity and fuzzy chaperone-substrate ensembles. eLife *6*, e28030.

Rüdiger, S., Germeroth, L., Schneider-Mergener, J., and Bukau, B. (1997). Substrate specificity of the DnaK chaperone determined by screening cellulose-bound peptide libraries. EMBO J. *16*, 1501–1507.

Sahasrabudhe, P., Rohrberg, J., Biebl, M.M., Rutz, D.A., and Buchner, J. (2017). The Plasticity of the Hsp90 Co-chaperone System. Mol. Cell *67*, 947–961.e5.

Sanchez, E.R., Meshinchi, S., Tienrungroj, W., Schlesinger, M.J., Toft, D.O., and Pratt, W.B. (1987). Relationship of the 90-kDa murine heat shock protein to the untransformed and transformed states of the L cell glucocorticoid receptor. J. Biol. Chem. *262*, 6986–6991.

Schlecht, R., Erbse, A.H., Bukau, B., and Mayer, M.P. (2011). Mechanics of Hsp70 chaperones enables differential interaction with client proteins. Nat. Struct. Mol. Biol. *18*, 345–351.

Schmid, D., Baici, A., Gehring, H., and Christen, P. (1994). Kinetics of molecular chaperone action. Science *263*, 971–973.

Schönfeld, H.J., Schmidt, D., Schröder, H., and Bukau, B. (1995). The DnaK chaperone system of Escherichia coli: quaternary structures and interactions of the DnaK and GrpE components. J. Biol. Chem. *270*, 2183–2189.

Schopf, F.H., Biebl, M.M., and Buchner, J. (2017). The HSP90 chaperone machinery. Nat. Rev. Mol. Cell Biol. *18*, 345–360.

Schowalter, D.B., Sullivan, W.P., Maihle, N.J., Dobson, A.D., Conneely, O.M., O'Malley, B.W., and Toft, D.O. (1991). Characterization of progesterone receptor binding to the 90- and 70-kDa heat shock proteins. J. Biol. Chem. *266*, 21165–21173.

Schröder, H., Langer, T., Hartl, F.U., and Bukau, B. (1993). DnaK, DnaJ and GrpE form a cellular chaperone machinery capable of repairing heat-induced protein damage. EMBO J. *12*, 4137–4144.

Schumacher, R.J., Hansen, W.J., Freeman, B.C., Alnemri, E., Litwack, G., and Toft, D.O. (1996). Cooperative action of Hsp70, Hsp90, and DnaJ proteins in protein renaturation. Biochemistry *35*, 14889–14898.

Sharma, S.K., De los Rios, P., Christen, P., Lustig, A., and Goloubinoff, P. (2010). The kinetic parameters and energy cost of the Hsp70 chaperone as a polypeptide unfoldase. Nat. Chem. Biol. *6*, 914–920.

Smith, D.F., Stensgard, B.A., Welch, W.J., and Toft, D.O. (1992). Assembly of progesterone receptor with heat shock proteins and receptor activation are ATP mediated events. J. Biol. Chem. *267*, 1350–1356.

Stankiewicz, M., Nikolay, R., Rybin, V., and Mayer, M.P. (2010). CHIP participates in protein triage decisions by preferentially ubiquitinating Hsp70-bound substrates. FEBS J. *277*, 3353–3367.

Taipale, M., Krykbaeva, I., Koeva, M., Kayatekin, C., Westover, K.D., Karras, G.I., and Lindquist, S. (2012). Quantitative analysis of HSP90-client interactions reveals principles of substrate recognition. Cell *150*, 987–1001.

Verba, K.A., Wang, R.Y., Arakawa, A., Liu, Y., Shirouzu, M., Yokoyama, S., and Agard, D.A. (2016). Atomic structure of Hsp90-Cdc37-Cdk4 reveals that Hsp90 traps and stabilizes an unfolded kinase. Science *352*, 1542–1547.

Wegele, H., Wandinger, S.K., Schmid, A.B., Reinstein, J., and Buchner, J. (2006). Substrate transfer from the chaperone Hsp70 to Hsp90. J. Mol. Biol. *356*, 802–811.

Xu, Z., Horwich, A.L., and Sigler, P.B. (1997). The crystal structure of the asymmetric GroEL-GroES-(ADP)7 chaperonin complex. Nature *388*, 741–750.

Xu, W., Mimnaugh, E., Rosser, M.F., Nicchitta, C., Marcu, M., Yarden, Y., and Neckers, L. (2001). Sensitivity of mature Erbb2 to geldanamycin is conferred by its kinase domain and is mediated by the chaperone protein Hsp90. J. Biol. Chem. *276*, 3702–3708.

Xu, W., Marcu, M., Yuan, X., Mimnaugh, E., Patterson, C., and Neckers, L. (2002). Chaperone-dependent E3 ubiquitin ligase CHIP mediates a degradative pathway for c-ErbB2/Neu. Proc. Natl. Acad. Sci. USA *99*, 12847–12852.

STAR★METHODS

KEY RESOURCES TABLE

REAGENT or RESOURCE	SOURCE	IDENTIFIER
Chemicals, Peptides, and Recombinant Proteins		
L-luciferin	SIGMA-Aldrich	Cat#L6882
Dexamethasone	SIGMA-Aldrich	Cat#D4902
Fluorescein-labeled dexamethasone (F-dex)	ThermoFisher Scientific	Cat#D1383
Radicicol	IRIS Biotech GmbH	Cat#LS1055
Protease inhibitor cOmplete, EDTA free	SIGMA-Aldrich	Ref. 05056489001
PMSF	SIGMA-Aldrich	Cat#P7626
IPTG	Fisher Bioreagents	Cat#BP1755
β-mercaptoethanol	SIGMA-Aldrich	Cat#M6250
DNase I	ThermoFisher Scientific	Cat#90083
Amylose Resin	NEB	Cat#8021S
Protino Ni-IDA resin	Macherey-Nagel	Ref. 745210
ATP	SIGMA-Aldrich	Cat#A2383
Critical Commercial Assays		
Pierce BCA Protein Assay Kit	ThermoFisher Scientific	Cat#23225
Experimental Models: Organisms/Strains		
MC1061	ThermoFisher Scientific	Cat#C66303
BL21(DE3) Star	ThermoFisher Scienfitic	Cat#C601003
BL21(DE3) Rosetta	Merck	Ref. 70954
XL10 Gold	Stratagene	Cat#200314
Recombinant DNA		
pCA528-dnaK	Schlecht et al., 2011	N/A
pMPM-A4-htpG-C10His	Graf et al., 2009	N/A
pDS56-luci	received from Bernd Bukau	N/A
pUHE21-2fdΔ12(dnaJ)	received from Bernd Bukau	N/A
pZE2-PzI-1(grpE)	received from Bernd Bukau	N/A
pCA528-hshsp70	Nguyen et al., 2017	N/A
pCA528-hshsp90β	Nguyen et al., 2017	N/A
pCA528-DNAJB1	Nguyen et al., 2017	N/A
pCA528-ydj1	Nguyen et al., 2017	N/A
pCA528-HSPA4	Rampelt et al., 2012	N/A
pMAL-c2E-GRLBD-F602S	Nguyen et al., 2017	N/A
pCA528-HOP	Nguyen et al., 2017	N/A
Software and Algorithms		
GraphPad Prism 6.0	GraphPad Software, Inc.	RRID: SCR_002798

CONTACT FOR REAGENT AND RESOURCE SHARING

Further information and requests for resources and reagents should be directed to and will be fulfilled by the Lead Contact, Stefan G. D. Rüdiger (s.g.d.rudiger@uu.nl).

METHOD DETAILS

Protein Purification

E. coli DnaK was purified according to a published procedure (Kityk et al., 2015). Briefly, DnaK was purified as native protein with an N-terminal His_6-Smt3-tag after overproduction in *ΔdnaK52* cells (BB1994). Cell pellets were resuspended in lysis buffer

(20 mM Tris/HCl pH 7.9, 100 mM KCl, 1 mM PMSF), subjected to lysis by microfluidizer EmulsiFlex C5 (Avestin, Ottawa, Canada), and afterward applied onto a column with Ni-IDA resin (Macherey-Nagel, Düren, Germany). Subsequently, the column was washed with 20 CV of lysis buffer and 10 CV of ATP buffer (20 mM Tris/HCl pH 7.9, 100 mM KCl, 5mM $MgCl_2$, 5 mM ATP), and 2 CV of lysis buffer. Proteins were eluted with elution buffer (20 mM Tris/HCl pH 7.9, 100 mM KCl, 250 mM imidazol). To remove the His_6-Smt3 tag from DnaK, the protein was treated with Ulp1 protease. After cleavage and dialysis into lysis buffer, the protein mixture was subjected again to a Ni-IDA column and the flow-through fraction containing tag-free DnaK was collected. Subsequently, DnaK was bound to an anion exchange column (Resource Q, GE Healthcare) equilibrated in low salt buffer (40 mM HEPES/KOH pH 7.6, 100 mM KCl, 5 mM $MgCl_2$). DnaK was eluted with a linear KCl gradient (0.1–1 M) within 10 CV.

E. coli DnaJ was purified according to a published procedure (Graf et al., 2009). Briefly, DnaJ was purified as native protein after overproduction in the *E. coli* strain W3110. Cell pellets were resuspended in lysis buffer (50 mM Tris/HCl pH 8, 10 mM DTT, 0.6% (w/v) Brij 58, 1 mM PMSF, 0.8 g/l Lysozyme) and lysed by microfluidizer EmulsiFlex-C5. Cell debris was removed by centrifugation at 20,000 g for 30 min. One volume of buffer A (50 mM sodium phosphate buffer pH 7, 5 mM DTT, 1 mM EDTA, 0.1% (w/v) Brij 58) was added to the supernatant and DnaJ was precipitated by addition of $(NH_4)_2SO_4$ to a final concentration of 65% (w/v). After centrifugation (15,000 g, 30 min), the ammonium sulfate pellet was dissolved in 220 mL buffer B (50 mM sodium phosphate buffer pH 7, 5 mM DTT, 1 mM EDTA, 0.1% (w/v) Brij 58, 2 M Urea) and dialysed against the 5 L buffer B. Subsequently, DnaJ was loaded onto a cation exchange column (SP-Sepharose, equilibrated with buffer B), washed with buffer B and eluted with a 15 CV long linear gradient of 0 to 666 mM KCl. DnaJ containing fractions were pooled and dialysed against 5 l buffer C (50 mM Tris/HCl, pH 7.5, 2 M urea, 0.1% (w/v) Brij 58, 5 mM DTT, 50 mM KCl). Afterward the sample was loaded onto a hydroxyapatite column equilibrated in buffer C. The column was first washed with 1 CV buffer C supplemented with 1 M KCl, and then with 2 CV of buffer C. DnaJ was eluted with a linear gradient (0%–50%, 1 CV) of buffer D (50 mM Tris/HCl, pH 7.5, 2 M urea, 0.1% (w/v) Brij 58, 5 mM DTT, 50 mM KCl, 600 mM KH_2PO_4) and 2 CV of 50% buffer D. The DnaJ containing fractions were pooled and dialysed against 2 L buffer E (50 mM Tris/HCl, pH 7.7, 100 mM KCl).

E. coli GrpE was purified as described before (Schönfeld et al., 1995). Briefly, GrpE was purified after overproduction in ΔdnaK52 cells (BB1994). Upon expression, cell pellets were resuspended in lysis buffer (Tris/HCl 50 mM, pH 7.5, 100 mM KCl, 3 mM EDTA, 1 mM PMSF) and lysed using a microfluidizer EmulsiFlex-C5. The lysate was clarified by centrifugation (18,000 g, 50 min). To the cleared lysate, ammonium sulfate (0.35 g/ml) was added, and insoluble proteins were separated from soluble by centrifugation (10,000 g, 20 min). The pellet was dissolved in 200 mL buffer A (50 mM Tris/HCl pH 7.5, 100 mM KCl, 1 mM DTT, 1 mM EDTA, 10% glycerol) and dialysed twice against the same buffer (3 l, 4 h). Subsequently, protein was loaded onto an anion exchange column (HiTrap Q XL; GE Healthcare) equilibrated with buffer A and GrpE was eluted using a linear gradient of buffer B (50 mM Tris/HCl pH 7.5, 1 M KCl, 1 mM DTT, 1 mM EDTA, 10% glycerol). Fractions containing the protein were dialyzed against buffer C (10 mM $K_xH_yPO_4$ pH 6.8, 1 mM DTT, 10% glycerol). On the following day the protein was loaded onto a Superdex 200 (GE Healthcare) gel filtration column equilibrated in buffer A, and concentrated using HiTrap Q XL with a steep gradient.

E. coli HtpG was purified as a native protein after overproduction in MC1061 cells induced by L-arabinose. Upon expression, cell pellets were resuspended in lysis buffer (25 mM $K_xH_yPO_4$ pH 7.2, protease inhibitor (cOmplete, EDTA free, Roche) and 5 mM β-mercaptoethanol). The cells were lysed by microfluidizer EmulsiFlex-C5 and the lysate was clarified by centrifugation (20,000 g, 40 min). The cleared lysate was loaded onto a Nickel column (Poros 20MC) and eluted with elution buffer (25 mM $K_xH_yPO_4$ pH 8, 400 mM NaCl, 500 mM imidazole, 5 mM β-mercaptoethanol). Eluted fractions were diluted in lysis buffer and loaded onto an anion exchange column (HiTrap Q XL). From this column, the protein was eluted using high salt buffer (50 mM $K_xH_yPO_4$ pH 7.2, 1 M KCl, 1 mM β-mercaptoethanol, 1 mM EDTA, 10% glycerol).

Human Hdj1 (DNJB1) was cloned and purified as a His_6-SUMO fusion as previously described (Malakhov et al., 2004) using buffer (40 mM HEPES/KOH pH 7.6, 150 mM KCl, 5 mM $MgCl_2$, 5% glycerol, 10 mM β-mercaptoethanol) and Ni-IDA material.

Human Hsp90α was expressed and purified as described earlier (Nguyen et al., 2017). Briefly, Hsp90α was expressed from the bacterial expression vector pCA528 (Andréasson et al., 2008) as fusion proteins with an N-terminal His_6-Smt3 tag in the *E. coli* strain BL21(DE3) Star/pCodonPlus (Invitrogen). After expression, cells were resuspended in lysis buffer (40 mM HEPES/KOH pH 7.5, 100 mM KCl, 5 mM $MgCl_2$, 10% glycerol, 4 mM β-mercaptoethanol, 5 mM PMSF, 1 mM Pepstatin A, 1 mM Leupeptin, and 1 mM Aprotinin) and lysed by a microfluidizer EmulsiFlex-C5. The lysate was clarified by centrifugation and incubated with Ni-IDA matrix. The matrix was loaded onto a column and washed with lysis buffer (without protease inhibitors) and eluted with lysis buffer containing 250 mM imidazole. Ulp1 was added to the eluted protein and the mixture was dialysed overnight against lysis buffer containing 20 mM KCl. The dialyzed protein was subjected to reverse Ni-IDA, followed by anion-exchange chromatography (ResourceQ; GE healthcare) with a linear gradient of 0.02-1 M KCl. Fractions of eluted Hsp90 were subjected to size exclusion chromatography on Superdex 200 in storage buffer (40 mM HEPES/KOH pH 7.5, 50 mM KCl, 5 mM $MgCl_2$, 10% glycerol, and 4 mM β-mercaptoethanol).

Human Hsp70 (gene name: HSPA1A; UniProt code: P0DMV8) was purified as native protein as an N-terminal His_6-Smt3 fusion after overproduction in BL21 (DE3) Rosetta cells. After harvesting by centrifugation, pelleted cells were resuspended in lysis buffer (20 mM Tris/HCl pH 7.9, 100 mM KCl, 1 mM PMSF) and lysed using microfluidizer EmusiFlex C5. The lysate was clarified by centrifugation (20,000 g, 50 min) and the supernatant was mixed with Ni-IDA beads and incubated for 15 min at 4°C. The lysate with beads was then poured into a column and was washed with 20 CV of lysis buffer (without PMSF), 20 CV of high salt buffer (20 mM Tris/HCl pH 7.9, 1 M KCl) and again with 2 CV of lysis buffer. The column was then slowly washed with 10 CV of ATP-buffer (40 mM Tris/HCl pH 7.9, 100 mM KCl, 5 mM $MgCl_2$, 5 mM ATP) to elute bound substrates. Hsp70 was eluted with twice 1 CV of elution buffer (40 mM

Tris/HCl pH 7.9, 100 mM KCl, 250 mM imidazole) and Ulp1 was added to the elution and dialyzed overnight against dialysis buffer (40 mM HEPES-KOH pH 7.6, 10 mM KCl, 5 mM $MgCl_2$). The dialysed sample was then loaded on Ni-IDA material, flow-through containing Hsp70 was collected and loaded onto a Resource Q anion exchange column. Hsp70 was eluted with a linear gradient of AEX elution buffer (40 mM HEPES/KOH pH 7.6, 1 M KCl, 5 mM $MgCl_2$, 10 mM β-mercaptoethanol, 5% glycerol) and dialysed against storage buffer (40 mM HEPES/KOH pH 7.6, 50 mM KCl, 5 mM $MgCl_2$, 10 mM β-mercaptoethanol, 10% glycerol).

Hop and Apg2 were purified as native proteins both as an N-terminal His_6-Smt3 fusion after overproduction in BL21 (DE3) Rosetta cells (Merck KGaA, Darmstadt, Germany). Upon expression, the cell pellets were resuspended in lysis buffer (40 mM Tris/HCl pH 7.9, 100 mM KCl, 5 mM ATP, 8 mg/l Pepstatin, 10 μg/ml Aprotinin, 5 mg/l Leupeptin). The cells were lysed by microfluidizer EmulsiFlex C5. The lysate was clarified by centrifugation (20,000 g, 40 min). After addition of Ni-IDA resin, the cleared lysate was incubated for 20 min, and then washed with 20 CV wash buffer (40 mM Tris/HCl pH 7.9, 100 mM KCl, 5 mM ATP) followed by elution with elution buffer (40 mM Tris/HCl pH 7.9, 100 mM KCl, 300 mM imidazole). Subsequently, buffer exchange was performed on a HiPrep 26/10 Desalting Column (GE Healthcare) equilibrated in the desalting buffer (20 mM Tris/HCl pH 7.9, 100 mM KCl, 10% glycerol). Upon buffer exchange, to remove the His-Smt3-tag, the protein was incubated overnight at 4°C with Ulp1 protease in the presence of 5 mM ATP. On the following day the protein was loaded onto a HiLoad 16/600 Superdex 200 Column equilibrated in gel filtration buffer (40 mM HEPES/KOH pH 7.6, 10 mM KCl, 5 mM $MgCl_2$, 10% glycerol). Protein containing fractions were pooled and subjected to anion-exchange chromatography on Resource Q column (GE Healthcare) for Apg2, and POROS 20HQ column (Thermo Fisher Scientific) in the case of Hop, both equilibrated with gel filtration buffer. In both cases the protein was eluted with linear KCl gradient (0.01–1 M) within 10 CV.

Photinus pyralis Firefly luciferase was purified according to previously described procedures (Rampelt et al., 2012). Briefly, firefly luciferase was expressed in XL10 Gold strain (Stratagene, US). Cells containing the expression plasmid were grown at 37°C until OD_{600} = 0.5 was reached, at which point the temperature was lowered to 20°C. After 45 min shaking at 20°C, cells were induced with IPTG overnight. After harvesting by centrifugation, pellets were resuspended in precooled lysis buffer (50 mM $Na_xH_yPO_4$ pH 8.0, 300 mM NaCl, 10 mM β-mercaptoethanol, protease inhibitors (cOmplete, EDTA free, Roche) DNase10 μg/ml) and lysed using a microfluidizer EmulsiFlex-C5. The lysate was cleared and incubated with Ni-IDA resin for 30 min. Subsequently, the lysate-protino mixture was loaded onto a column and washed with 10 CV of lysis buffer, 10 CV of wash buffer (50 mM $Na_xH_yPO_4$ pH 8.0, 300 mM NaCl and 10 mM β-mercaptoethanol) and eluted by addition of elution buffer (50 mM $Na_xH_yPO_4$ pH 8.0, 300 mM NaCl, 250 mM Imidazole, 5 mM β-mercaptoethanol) collecting 1-2 mL fractions. Luciferase was dialyzed overnight using dialysis buffer (50 mM $Na_xH_yPO_4$ pH 8.0, 300 mM NaCl and 10 mM β-mercaptoethanol, 10% glycerol). All data points were pipetted in triplicates and the experiments were reproduced with different luciferase batches.

Saccharomyces cerevisiae Ydj1 was overproduced as native protein in *E. coli* from an IPTG-inducible expression plasmid. After addition of IPTG, cells were grown for additional 5 h. Cells were harvested by centrifugation, washed twice with H_2O and resuspended in a minimal volume of 1x lysis buffer (10x lysis buffer: 180 mM Spermidin/HCl pH 7.6, 1 M $(NH_4)_2SO_4$, 50 mM DTT, 5 mM EDTA) in buffer A (50 mM Tris/HCl, pH 7.6, 10% (w/w) saccharose, 1 mM PMSF). Cells were disrupted in a microfluidizer EmulsiFlex-C5 and cell debris removed by centrifugation. $(NH_4)_2SO_4$ was added to the clarified lysate to a saturation of 85% over a 30-min period and stirring was continued for an additional 30 min at 4°C. Ydj1 was separated from precipitated proteins by centrifugation (20 min; 15,000 g) and dialyzed overnight against Ydj1 buffer (HEPES/KOH 40 mM pH 7.6, 150 mM KCl, 1 mM DTT, 5% glycerol). The protein was then loaded onto an anion exchange column (DEAE-Sepharose), washed with Ydj1 buffer and eluted with a linear gradient of 0-800 mM KCl over 3 CV. The fractions containing Ydj1 were collected, concentrated and loaded onto a Superdex 200 and subsequently loaded onto a ResourceQ column for further purification and concentration. Ydj1 was stored in Ydj1 buffer.

For purification of human GR-LBD (glucocorticoid receptor ligand-binding domain), the protocol previously described (Nguyen et al., 2017) was followed. Briefly, the GR-LBD fragment (residues 521-777 of human glucocorticoid receptor) with an F602S amino acid exchange was produced as fusion to the maltose binding protein (MBP) in BL21(DE3) Star Rosetta. Cells containing the expression plasmid were grown at 37°C until OD_{600} = 0.8 was reached. Dexamethasone was then added to a final concentration of 250 μM and cells were induced with 0.5 mM IPTG at 18°C overnight. Cells were lysed using a microfluidizer EmulsiFlex-C5 in MBP-lysis buffer (50 mM Tris HCl pH 8.3, 300 mM KCl, 5 mM $MgCl_2$, 0.04% CHAPS, 1 mM EDTA, 10% glycerol, 50 μM dexamethasone, 5 mM β-mercaptoethanol) with protease inhibitor cOmplete tablets (Roche) and purified using an amylose resin (NEB, E8021S) following the manufacturer protocol with 50 μM dexamethasone addition to every buffer. To remove dexamethasone the eluted protein was dialysed in 2 l MBP-lysis buffer (without dexamethasone) four times, each at least 2 h. Protein was freshly purified before use.

Luciferase Refolding Assay

For refolding by the bacterial Hsp70 system, firefly luciferase (10 μM) was chemically denatured by incubation in unfolding buffer (5 M GdmCl, 30 mM Tris/acetate pH 7.5) for 10 min at 22°C. For refolding, luciferase was diluted 125-fold into refolding buffer (25 mM HEPES/KOH pH 7.6, 100 mM KOAc, 10 mM $Mg(OAc)_2$, 2 mM ATP, 5 mM DTT) (80 nM final luciferase concentration), containing the specified chaperone concentrations and incubated at 30°C. Luciferase activity was determined by photon counting in a Lumat LB 9507 luminometer (Berthold Technologies) by transferring 1 μL of sample to 124 μL of assay buffer (100 mM K-phosphate buffer pH 7.6, 25 mM Glycylglycine, 100 mM KOAc, 15 mM $Mg(OAc)_2$, 5 mM ATP) at the indicated time points and mixing with 125 μL of 80 μM luciferin injected by the instrument right before each measurement. Luminescence was measured for 5 s.

For the human system, 80 nM firefly luciferase in refolding buffer containing the indicated amounts of chaperones was heat-denatured at 42°C for 10 min. At the indicated time points, 1 μL sample was diluted into 124 μL of assay buffer and measured as described for the bacterial system. Refolding yields were normalized based on the activity of non-denatured luciferase.

Our initial conditions (before titration) compare with the previous conditions used in literature in the following way:

Source	[Luciferase] (nM)	[DnaK] (μM)	Ratio (DnaK/DnaJ/GrpE)
This paper	80	0.8	10:2:5
Bischofberger et al., 2003	100	1.0	10:1:5
Sharma et al., 2010	100	1.0	10:1:5
Kityk et al., 2015	80	0.8	10:2:5
Genest et al., 2011	80	0.75	10:2:0.7
Buchberger et al., 1996	80	1.2	10:1:5

Luciferase Data Fitting

All data fitting was performed in GraphPad Prism 6.0 (GraphPad software, La Jolla CA, USA). Refolding kinetics (Figures 1B, 2A, and 3A) were fitted with a single exponential equation $y = y_{max} \cdot (1 - e^{-k \cdot t})$ individually. Since no statistical differences were found between the rates for the different Hsp70 concentrations, the data were also globally fitted using a single (shared) rate constant k but different y_{max}.

Reaction rates k and their standard error from the fit of data in Figures 1B, 2A, and 3A to a one phase association equation.

	k (s^{-1})	±SEM
Figure 1B	0.093	0.004
Figure 2A	0.115	0.006
Figure 3A	0.033	0..002

For each concentration, the percentage of refolded luciferase at the plateau were extrapolated from the fits and standard error of the fit for the plateau were calculated:

Plateau values and their standard error from the fit of data in Figures 1B, 2A, and 3A.

To fit the refolding yield versus Hsp70 concentration data (Figures 1C, 3B) we derived an equation from a chemical reaction scheme shown in detail in the next methods section (Equation System):

Figure 1B		
[DnaK] μM	y_{max} (% refolded)	±SEM
0	7.35	0.27
0.8	59.66	1.51
1	64.26	1.42
1.5	71.77	1.11
2	83.49	1.79
4	59.28	1.21
6	36.14	0.81
8	23.67	0.42
10	10.79	0.26

Figure 2A		
[DnaK] μM	y_{max} (% refolded)	±SEM
0	1.01	0.03
0.8	35.73	1.38
1	40.88	0.99
1.5	50.49	1.09
2	77.80	1.53
4	89.14	3.75
7	52.53	1,58
8	13.78	0.77
10	8.18	0.71

Figure 3A		
[Hsp70] μM	y_{max} (% refolded)	±SEM
0	14.36	0.29
1	66.04	2.34
2	83.41	2.36
4	61.09	1.08
8	33.36	1.45
12	13.50	1.09

$$A_n = \frac{\left(\frac{k_f K_2 [H] - k_a [H]^3}{K_1 K_2 + K_2 [H] + [H]^2} + r_s\right)[C_d]_0}{(r_n + r_s)} \quad (1)$$

With A_n, % refolding yield; k_f, actual folding rates (s^{-1}); k_a, actual rate for the conversion of the client into the non-refoldable state; [H], Hsp70 concentration (μM); K_1, dissociation equilibrium constant for the Hsp70-client complex (μM); K_2, dissociation equilibrium constant for the Hsp70-client-Hsp70 complex (μM); $[C_d]$, relative concentration of the denatured protein at time point 0 (= 100%); r_n, observed refolding rate (s^{-1}); r_s, apparent rate of the side reaction to the non-refoldable state of the client. A stable result was obtained when assuming that the numerical value for k_a and r_s are identical.

Values of the parameters of the derived equation used in Figures 1C and 3B.

	Figure 1C	Figure 3B
$[C_d]_0$ (%)	100.0	100.0
r_n (s^{-1})	0.093	0.033
k_f (s^{-1})	0.727	0.157
K_1 (μM)	9.231	4.805
K_2 (μM)	0.462	0.879
r_s (s^{-1})	0.003	0.001
k_a (s^{-1})	0.003	0.001
correlation r^2	0.986	0.958

Equation (1) assumes Hsp70 concentration as constant since it is in large excess over the client. In the situation of Figure 2B, not only Hsp70 concentration changes but its co-chaperones are titrated up as well. DnaJ was shown to bind as a client to DnaK when no other clients are present or, presumably, when in large excess over the client (Laufen et al., 1999). That translates in a more complex situation that could not be described by the same equation. In this case, a dotted line was used to guide the eye.

For the Hsp90 titrations, % refolding versus time data were fitted to a single exponential equation as described for the Hsp70 experiments with a shared rate k (graphs not shown). Refolding versus [Hsp90] was fitted to a single exponential equation with association constant K (μM^{-1}) (Figures 1D, 2D, 3C).

$$\%\ Refolding = \%Ref_0 + (Plateau - \%Ref_0) * \left(1 - e^{-K*[Hsp90]}\right)$$

Values of the parameters of the single exponential equation used to fit data in Figures 1D, 2D, 2F, and 3C (Hsp90 titration experiments).

	Figure 1D	Figure 2D	Figure 2F	Figure 3C
Plateau (% refolded)	80.37	87.60	72.36	91.08
K (μM^{-1})	6.905	3.020	2.080	0.8803
correlation r^2	0.9626	0.9863	0.9325	0.9040

Equation System

Analysis of the refolding yield of denatured luciferase in the presence of excess Hsp70: Scheme 1 illustrates the simplest version of the refolding reaction that is able to explain our observations. The denatured client (C_d) interacts with Hsp70 (H) to form the Hsp70·client (HC_d) complex. The Hsp70·client complex can dissociate, and the client refold into the native state (C_n) with the rate constant k_f. At high concentrations of Hsp70 the Hsp70·client complex could react with a second Hsp70 molecule to give the trimeric complex Hsp70·client·Hsp70 (H_2C_d). This complex could associate with a third Hsp70 molecule with reaction rate k_a to give a client state (H_3C_d*) that is inactive and not readily refolded. At high concentrations of Hsp70, a side reaction of the denature client to aggregates is unlikely and therefore neglected. For simplification, the reactions of the co-chaperones, J-domain protein and the nucleotide exchange factor, were disregarded.

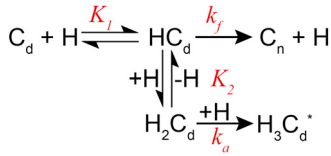

C_d, denatured client; C_d*, denatured client that is not readily refolded; C_n, native active client; H, Hsp70; K_1, dissociation equilibrium constant for association of Hsp70 with client; K_2, dissociation equilibrium constant for association of a second Hsp70 molecule with the client; k_f, folding rate constant; k_a, rate for the conversion of the client into a not readily refoldable conformation. Under the conditions of the experiments native client remains native. The reaction to the native state is essentially irreversible. The reaction to the H_3C_d* conformation is modeled for simplicity also as irreversible reaction. Changing this reaction into a reversible reaction will not lead to a decrease in final yield of native protein with increasing Hsp70 concentrations as observed in our experiments but to a decrease in folding rates. The H_3C_d* state is most likely a heterogeneous unfolded state with several Hsp70 proteins bound whereby any Hsp70 dissociating is immediately replaced by another Hsp70 associating with this state creating a practically irreversible situation.

From the chemical equation follows for the equilibrium constants:

$$K_1 = \frac{[H][C_d]}{[HC_d]} \Leftrightarrow [HC_d] = \frac{[H][C_d]}{K_1} \tag{1}$$

$$K_2 = \frac{[HC_d][H]}{[H_2C_d]} \Leftrightarrow [H_2C_d] = \frac{[HC_d][H]}{K_2} = \frac{[C_d][H]^2}{K_1K_2} \tag{2}$$

Since Hsp70 is in large excess over client, its concentration remains roughly constant during the reaction and is equal to the concentration added at the beginning.

$$[H] \approx [H]_0 = const.$$

The concentration of the denatured client is equal to the concentration added at the beginning ($[C_d]_0$) minus the concentrations of native and Hsp70 containing client complexes.

$$[C_d] = [C_d]_0 - [HC_d] - [H_2C_d] - \left[H_3C_d^*\right] - [C_n] \tag{3}$$

With (1) and (2):

$$[C_d] + \frac{[H]}{K_1}[C_d] + \frac{[H]^2}{K_1K_2}[C_d] = [C_d]_0 - \left[H_3C_d^*\right] - [C_n]$$

$$[C_d] = \frac{[C_d]_0 - [H_3C_d^*] - [C_n]}{1 + \frac{[H]}{K_1} + \frac{[H]^2}{K_1K_2}} \tag{4}$$

The regain in client activity depends on the refolding rate of the client and the concentration of the Hsp70·client complex:

$$\frac{d[C_n]}{dt} = k_f \bullet [HC_d] = k_f \bullet \frac{[H][C_d]}{K_1}$$

$$\frac{d[C_n]}{dt} = k_f \bullet \frac{[H]([C_d]_0 - [H_3C_d^*] - [C_n])}{K_1\left(1 + \frac{[H]}{K_1} + \frac{[H]^2}{K_1K_2}\right)} = k_f \bullet \frac{K_2[H]([C_d]_0 - [H_3C_d^*] - [C_n])}{K_1K_2 + K_2[H] + [H]^2}$$

$$k_f' := \frac{k_fK_2[H]}{K_1K_2 + K_2[H] + [H]^2} \tag{5}$$

$$\frac{d[C_n]}{dt} = k_f'[C_d]_0 - k_f'[H_3C_d^*] - k_f'[C_n]$$

$$\frac{d[C_n]}{dt} + k_f'[C_n] + k_f'[H_3C_d^*] - k_f'[C_d]_0 = 0 \tag{6}$$

The formation of the $(Hsp70)_3$-client complex depends on the concentration of Hsp70 and of the $(Hsp70)_2$-client complex:

$$\frac{d[H_3C_d^*]}{dt} = k_a \bullet [H_2C_d][H] = k_a \bullet \frac{[C_d][H]^3}{K_1K_2}$$

$$\frac{d[H_3C_d^*]}{dt} = k_a \bullet \frac{[H]^3}{K_1K_2} \bullet \frac{[C_d]_0 - [H_3C_d^*] - [C_n]}{1 + \frac{[H]}{K_1} + \frac{[H]^2}{K_1K_2}} = k_a \bullet [H]^3 \bullet \frac{[C_d]_0 - [H_3C_d^*] - [C_n]}{K_1K_2 + K_2[H] + [H]^2}$$

$$k_a' := \frac{k_a[H]^3}{K_1K_2 + K_2[H] + [H]^2} \tag{7}$$

$$\frac{d[H_3C_d^*]}{dt} = k_a'[C_d]_0 - k_a'[H_3C_d^*] - k_a'[C_n]$$

$$\frac{d[H_3C_d^*]}{dt} + k_a'[C_n] + k_a'[H_3C_d^*] - k_a'[C_d]_0 = 0 \tag{8}$$

Equation (6) minus (8) yields:

$$\frac{d[C_n]}{dt} - \frac{d[H_3C_d^*]}{dt} + (k_f' - k_a')[C_n] + (k_f' - k_a')[H_3C_d^*] - (k_f' - k_a')[C_d]_0 = 0 \tag{9}$$

A general solution for this type of differential equation is:

$$[C_n] = A_n\left(1 - e^{-r_nt}\right) \tag{10}$$

$$[H_3C_d^*] = A_S\left(1 - e^{-r_St}\right) \tag{11}$$

with A_n and r_n are equal to yield and apparent rate of the refolding reaction and A_s and r_s are equal to the yield and apparent rate of the side reaction to the not refoldable state $H_3C_d^*$ of the client.

$$\frac{d[C_n]}{dt} = A_n r_n e^{-r_n t} \tag{12}$$

$$\frac{d[H_3C_d^*]}{dt} = A_S r_S e^{-r_S t} \tag{13}$$

Inserting Equations (10) to (13) into (9):

$$A_n r_n e^{-r_n t} - A_S r_S e^{-r_S t} + (k_f' - k_a')A_n\left(1 - e^{-r_n t}\right) + (k_f' - k_a')A_S\left(1 - e^{-r_S t}\right) - (k_f' - k_a')[C_d]_0 = 0 \tag{14}$$

At the beginning of the reaction no native and no $(Hsp70)_3$-client complex is present:

$$For:\ t = 0 \Rightarrow [C_n] = 0,\ [H_3C_d^*] = 0,\ e^0 = 1$$

$$A_n r_n - A_S r_S - (k_f' - k_a')[C_d]_0 = 0$$

$$A_n r_n - A_S r_S = (k_f' - k_a')[C_d]_0 \tag{15}$$

At the end of the reaction all client proteins are either converted into the native state or into the not refoldable state.

$$For:\ t \to \infty \Rightarrow [C_n] + [H_3C_d^*] = [C_d]_0 \Rightarrow [C_d]_0 = A_n\left(1 - e^{-r_n \infty}\right) + A_S\left(1 - e^{-r_S \infty}\right) = A_n + A_S$$

$$A_S = [C_d]_0 - A_n \tag{16}$$

Since we directly measure the activity of the native client, which is proportional to its amount, we eliminate A_s from Equation (15) using (16) and solve the equation to yield A_n:

$$A_n r_n - [C_d]_0 r_s + A_n r_s = (k_f' - k_a')[C_d]_0$$

$$A_n(r_n + r_s) = (k_f' - k_a' + r_s)[C_d]_0$$

$$A_n = \frac{(k_f' - k_a' + r_s)[C_d]_0}{(r_n + r_s)} \tag{17}$$

With Equations (5) and (7) we get:

$$A_n = \frac{\left(\frac{k_f K_2[H]}{K_1K_2 + K_2[H] + [H]^2} - \frac{k_a[H]^3}{K_1K_2 + K_2[H] + [H]^2} + r_s\right)[C_d]_0}{(r_n + r_s)}$$

$$A_n = \frac{\left(\frac{k_f K_2[H] - k_a[H]^3}{K_1K_2 + K_2[H] + [H]^2} + r_s\right)[C_d]_0}{(r_n + r_s)} \tag{18}$$

Equation (18) was used to fit the yield of luciferase refolding at different Hsp70 concentrations. To reduce the number of parameters during the nonlinear fitting procedure and because the apparent refolding rates were equal at all Hsp70 concentrations, we determined r_n from the refolding kinetics by global fitting of all data and used it as a constant in the fit of the yield data. While fitting these data we found that a stable result was obtained when assuming that the numerical value for k_a and r_s are identical.

GR-LBD Fluorescence Polarization Assay

Fluorescence polarization of fluorescein-labeled dexamethasone (F-Dex) was measured in a plate reader (CLARIOStar, BMG Labtech) with excitation/emission wavelengths of 485/538 nm using a 384-well black flat-bottom microplate (Corning). GR-LBD (2 μM) was denatured at 42°C for 10 minutes in Tris-HCl buffer pH 8.3, 300 mM KCl, 5 mM β-mercaptoethanol, 5 mM $MgCl_2$ and 2 mM ATP in

the absence or presence of 15 μM Hsp70 and 2 μM Ydj1. After denaturation in the indicated samples, 15 μM Apg2, 10 μM Hsp90, 5 μM Hop were added. F-Dex was added to a final concentration of 20 nM and ligand association was monitored measuring fluorescence polarization over time until plateau was reached. Control samples of GR-LBD alone were prepared with matching volumes of the chaperones storage buffer. Data was normalized to 100% and 0% binding of F-Dex considering the folded and unfolded GR-LBD samples, respectively. GraphPad Prism 6.0 was used to plot the data.

QUANTIFICATION AND STATISTICAL ANALYSIS

All biochemical assays were performed at least 3 times independently. Data were analyzed with GraphPad Prism 6.0 (GraphPad Software).